Environmental Modelling and Software 112 (2019) 36–45

Contents lists available at ScienceDirect

Environmental Modelling & Software

journal homepage: www.elsevier.com/locate/envsoft

Optimal salinity and water level control of water courses using Model Predictive Control

Boran Ekin Aydin[a,*], Xin Tian[a], Joost Delsman[b], Gualbert H.P. Oude Essink[b,c], Martine Rutten[a], Edo Abraham[a]

[a] Department of Water Management, Delft University of Technology, 2628CN, Delft, the Netherlands
[b] Department of Subsurface and Groundwater, Deltares, P.O. Box 85467, 3508 AL, Utrecht, the Netherlands
[c] Department of Physical Geography, Utrecht University, 3584 CS, Utrecht, the Netherlands

A B S T R A C T

Worldwide, delta areas are under stress due to climate change. With rising sea levels and decreasing freshwater availability, surface water salinization due to groundwater exfiltration is expected to increase in these low-lying areas. To counteract surface water salinization, freshwater diverted from rivers is used to flush agricultural ditches. In this paper, we demonstrate a Model Predictive Control (MPC) scheme to control salinity and water levels in a water course while minimizing freshwater usage. A state space description of the discretized De Saint Venant and advection-dispersion equations for water and salt transport, respectively, is used as the internal model of the controller. The developed MPC scheme is tested using groundwater exfiltration data from two different representative Dutch polders. The tests demonstrate that water levels and salinity concentrations can successfully be controlled within set limits while minimizing the freshwater used.

Software and data availability

The developed MPC scheme is implemented in MATLAB. Please contact the corresponding author for further information and availability. Year first available: March 2018. Software required: MATLAB.

1. Introduction

Salinization of polders is often caused by exfiltration of saline groundwater (Hof and Schuurmans, 2000). Land subsidence, climate change and sea level rise accelerate salinization by enhancing the intrusion rate (Oude Essink et al., 2010). In low-lying delta areas as the Rhine-Meuse delta of the Netherlands, saline groundwater will increasingly move towards the ground surface and exfiltrate to the surface water system (Delsman et al., 2014a). Saline water threatens agricultural activities and the freshwater ecosystem in the polders (A polder is an artificially drained catchment in which the surface water level in the ditch network is regulated by pumping). Therefore, salinity control is necessary for both agricultural purposes and maintaining certain freshwater ecosystems (Hof and Schuurmans, 2000). To maintain acceptable surface water quality, freshwater diverted from rivers is used for flushing the canals and ditches in coastal areas.

In the Netherlands, the largest saline groundwater exfiltration to the surface water are found in deep polders (de Louw et al., 2013). Freshwater from the rivers Rhine and Meuse is used for flushing these polders during agricultural growing season. This surface water flushing amounts to 15% of the total freshwater demand in the Netherlands (Klijn et al., 2012). However, decreasing freshwater availability (Forzieri et al., 2014) and expected increase of surface water salinization (Delsman et al., 2014a; Oude Essink et al., 2010) forces water managers to reconsider the current water management practice in deep polders. Increasing the efficiency of surface water flushing is regarded as a promising way to decrease surface water demand (Delta Programme Commissioner, 2014).

Efficient water management in polders is a challenging process since the water level should be kept within a narrow margin, excess water is drained to the ditches with a fast response time while the saline groundwater exfiltration potentially increases the salinity in the top layer/triggers the salinization problem. Saline groundwater exfiltrates to the polder ditch through boils (direct pathways between aquifer and the surface water), drains (exfiltration of shallow phreatic groundwater) and ditches (diffusive seepage below the ditch itself) (Delsman et al., 2013). When the salinity level in the polder ditch exceeds a certain threshold, freshwater is introduced through the upstream structure of the ditch to flush the surface water system. However, current practice of salinity control in polders generally involves constant flushing during the growing season, manually opening the inlet culverts at the start and closing them at the end of the growing season (Delsman, 2015). Water level control is achieved by the operation of a pumping station, responding to water level measurements near the

* Corresponding author. Department of Water Management, Delft University of Technology, 2628CN, Delft, the Netherlands.
E-mail address: B.E.Aydin@tudelft.nl (B.E. Aydin).

https://doi.org/10.1016/j.envsoft.2018.11.010
Received 23 March 2018; Received in revised form 19 November 2018; Accepted 19 November 2018
Available online 20 November 2018
1364-8152/

pumping station. Flushing is generally not considered in operation and this may result in excess use of freshwater and unnecessary pumping (Delsman, 2015).

In this paper, we demonstrate a Model Predictive Control (MPC) scheme for optimal operation of a water course or called here test polder ditch (Fig. 2) for flushing by explicitly considering freshwater conservation. The focus of our research is to find a solution for supplying the available freshwater resources in a more efficient way for real polders. To the best knowledge of the authors, previous studies controlling water level and water quality did not consider the amount of freshwater supply. Xu et al. (2013) merely mentioned 'over-flushing' as an important topic in their discussion. Therefore, in this study we proposed a solution to this problem by introducing an additional control objective as the minimization of freshwater use and demonstrated how much freshwater can be saved if flushing is done only when it is necessary. Another novelty of this paper is using physically-based models in real time control, as opposed to low order numerical models derived using proper orthogonal decomposition (POD). We employed the discretized Saint Venant (SV) and advection dispersion (AD) equations as the internal model of the real time controller. Finally, we coupled an exfiltration model with the controller to deal with real exfiltration scenarios driven by real precipitation and hydrological data instead of using arbitrary exfiltration flux and concentration. All these three aspects of this paper are important steps for application of the developed MPC scheme to a real polder system in a follow-up research.

An internal model employed a coarse discretization of SV and AD equations. A detailed state space description is given in section 3. For the simulations, we solved the discretized SV and ADE equations programmed in MATLAB (The Mathworks Inc, 2016). We tested the developed control scheme in closed-loop simulations for two representative Dutch polders with different saline groundwater exfiltration characteristics (Fig. 1). As described in Section 2.2 the simulation models are abstractions of real-world ditches (Schermer polder (Delsman et al., 2017) and Lissertocht catchment (Delsman et al., 2013)) and are used to simulate the system dynamics based on discretized SV and AD equations, where the scenarios are designed with real precipitation and hydrological data for the areas using the Rapid Saline Groundwater Exfiltration Model (RSGEM). The Lissertocht catchment (surface level 6–3.5 m below sea level (BSL), water depth 6.4 m BSL, salinity concentration variation in the ditches 136–5453 g/m^3 (Delsman et al., 2013)) represents of deep polders, where the main salinity input is deep saline groundwater exfiltration through boils (de Louw et al., 2010) (Fig. 1c). In this catchment, two different layouts are observed: main ditches that receives the drained water directly from the drains and main ditches without drain connection but connected to stagnant ditches (collected excessive water in the surrounding area is drained to these stagnant ditches). We considered both layouts in this

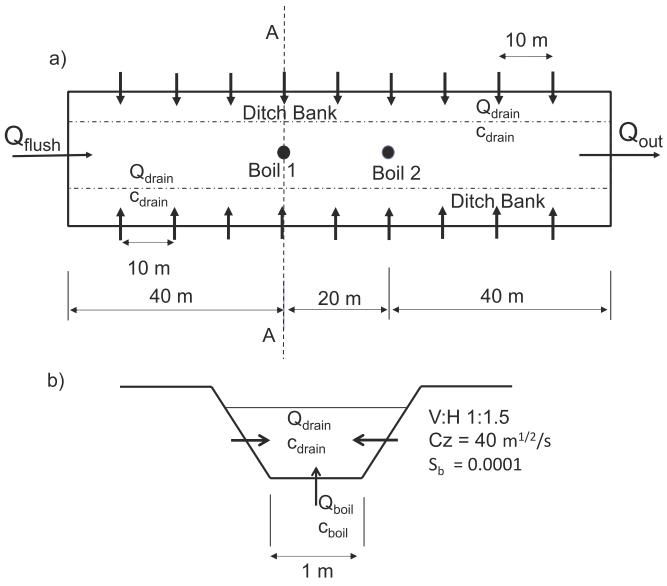

Fig. 2. a. Schematization of the test polder ditch (not to scale) for the first scenario, 10 m drainage spacing, 1 m bed width, 1:1.5 side slope, Chezy coefficient 40 m$^{1/2}$/s and bottom slope 0.0001 [-] with flushing discharge (Q_{flush}), outflow discharge (Q_{out}), groundwater drain exfiltration discharge (Q_{drain}) and concentration (c_{drain}), locations of the two boils and two locations used in controller design that are 40 m and 60 m downstream of the flushing inlet, b. Cross section of the ditch (A-A in (a)) with drain exfiltration discharge (Q_{drain}) and concentration (c_{drain}), boil discharge (Q_{boil}) and concentration (c_{boil}).

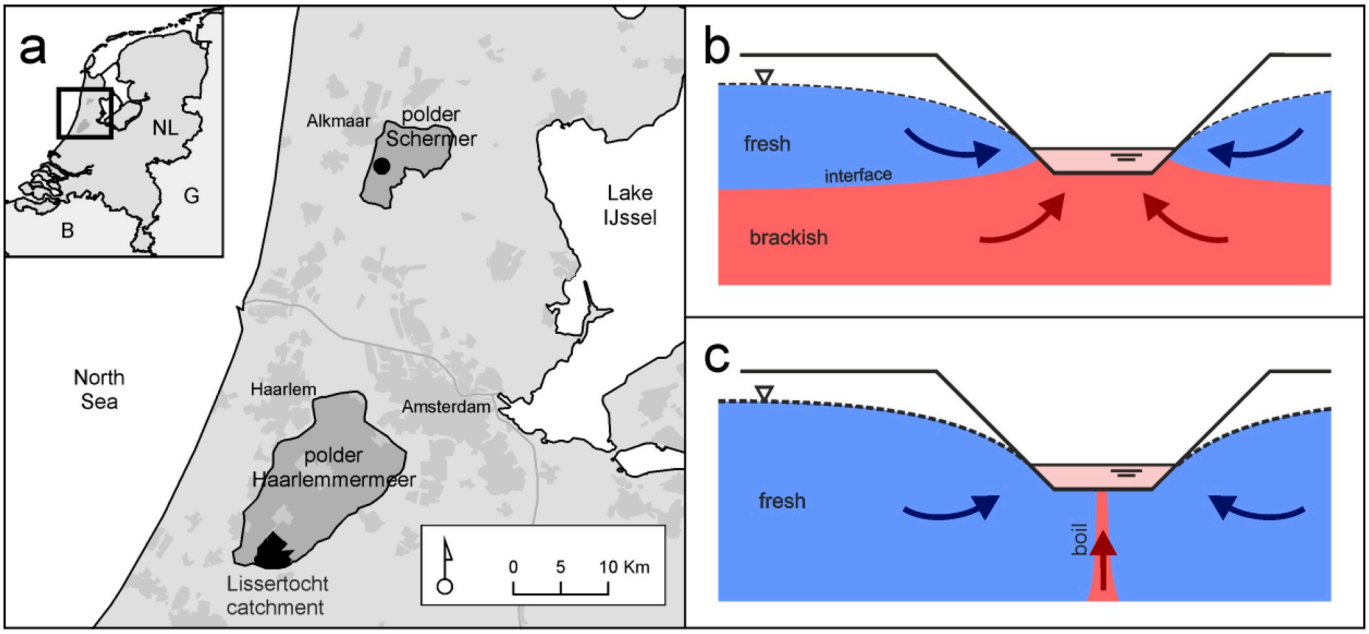

Fig. 1. a) Locations of the two polders in the Netherlands used for testing the developed MPC scheme: i) Schermer Polder, ii) Lissertocht Catchment (adapted from Delsman, 2015), **b)** conceptualization of fresh and brackish groundwater flow to a ditch in the Schermer Polder, and **c)** conceptualization of fresh and brackish groundwater flow and a boil connecting the deep saline aquifer to a ditch in the Lissertocht catchment.

study. On the other hand, the Schermer polder (surface level 4.14–3.86 m BSL, water depth average depth, water depth 5 m BSL, salinity concentration variation in the ditches 700–7700 g/m^3 (Delsman et al., 2014b)) is representative of polders where the main salinity input derives from shallow saline groundwater, viz. exfiltrating towards ditches and tile drains (Fig. 1b). Interested readers are referred to Delsman et al., 2017, 2013) for further information about the areas considered in this study. The saline groundwater exfiltration is modelled by the RSGEM (Delsman et al., 2017).

Water systems have hydraulic structures like weirs, gates and pumps in place. To control the water quantity and quality these structures have to be operated according to the desired state of the system. Operational water management aims to optimize the control of these structures by means of Real Time Control (RTC). Over the past decades, RTC techniques have been used in the field of operational water management to control water volumes and levels, such as feedback controller (Clemmens and Wahlin, 2004; Schuurmans, 1997), feedforward controller (Bautista et al., 2003) or Model Predictive Control (MPC) (Aydin et al., 2016; Delgoda et al., 2016; Horváth et al., 2015; Tian et al., 2017, 2016; van Overloop et al., 2014). Over about the past 15 years, water quality control has also been considered. Several examples are: an adaptive control to restrict algae development in a canal (Litrico et al., 2011); a dynamic control to prevent salt intrusion in a lake (Augustijn et al., 2011); a genetic algorithm to control the water quality of a waste water system (Fu et al., 2008) and to control regional wastewater treatment (Cho et al., 2004); different combinations of proportional integral derivative control with MPC to control pollutants in a river (Puig et al., 2014); and an MPC scheme to control water quantity and quality in a polder (Xu et al., 2013, 2010).

MPC uses an internal model to predict the states of the surface water system over the prediction horizon. The accuracy of the internal model affects the control performance of the MPC in terms of accuracy and computation time (Xu, 2016). Simple models exist for water quantity control like Integrator Delay model (Schuurmans et al., 1995) and Integrator Resonance model (van Overloop et al., 2014). For water quality control, Xu et al. (2010, 2013) used a simple reservoir model assuming full mixing to control the average salinity concentration in a ditch and proceeded by applying a model reduction technique and achieve a simple internal model decreasing computational time requirements to control the downstream water salinity concentration. Moreover, no previous studies pay attention to the minimal freshwater use of polder flushing assuming an unlimited source. Decreasing the freshwater intake to the ditch for flushing will directly decrease the amount of pumping water from the system. This is considered as a surrogate for saving energy. Therefore, in this study we develop a scheme to regulate water level and salinity of a test polder ditch by minimizing the freshwater use. We present an internal model and a state space description for a MPC scheme to control the flushing of the ditch. Multiple objectives (water level and salinity control and minimization of freshwater use) while meeting the constraints of the system are satisfied. We use the discretized SV and ADE equations as the internal model for the controller which enables us to regulate the water level and salinity concentration in any discretization point of the test polder ditch.

2. Modelling for the simulations

In this section, we described the groundwater exfiltration model used to estimate the ditch and drain exfiltration to the ditch, and the models used for the simulation of the flushing of a ditch.

2.1. Modelling the saline groundwater exfiltration - RSGEM

Saline groundwater exfiltration in low-lying polders is governed by the regional hydraulic gradient in the upper groundwater system. Saline groundwater moves upward and mixes with the surface water, increasing the salinity of the surface water. Existing groundwater models require long run times and limit the application in operational freshwater management. To support operational water management of freshwater resources in coastal lowlands, Delsman et al. (2017) formulated a hydro(geo)logical model for fast calculation of groundwater exfiltration flux and salinity in a low-lying catchments. RSGEM recognizes that groundwater exfiltration salinity critically depends on both the fast-responding pressure distribution, and the slow-responding salinity distribution in the shallow groundwater. The model was developed for a test site in Schermer polder, and was validated using both measured groundwater levels, exfiltration rates and salinity response and results of a previously applied detailed, complex model to the same area (Delsman et al., 2017). RSGEM is a lumped water balance model used for determining the saline groundwater ditch and drain exfiltration discharges and salinity concentrations. The model aimed to include the saline groundwater exfiltration dynamics in coastal lowlands and is suitable for densely drained polders where fresh rainwater overlies shallow saline groundwater. RSGEM uses precipitation, evaporation and groundwater levels as the input and the output is the groundwater exfiltration concentration (Figs. 5a and 7a) and discharge (Figs. 5b and 7b). Other parameters necessary for running RSGEM for the given cases are taken from Delsman et al. (2013, 2017). Interested readers can refer to Delsman et al. (2017) for detailed information about RSGEM.

In this study, we forced RSGEM with real-world data (precipitation, evaporation and groundwater levels) from two Dutch polders (Schermer polder (Delsman et al., 2017) and Lissertocht catchment (Delsman et al., 2013)) to obtain realistic exfiltration scenarios. The modeled exfiltration discharge and the concentration are used as known disturbance for the developed controller. We assumed full system knowledge and perfect predictions for the exfiltration calculated by the RSGEM, thus, no uncertainty assessment is conducted.

2.2. Modelling the flushing of a polder ditch

To model the flushing of a polder ditch, transport of water and transport of dissolved matter have to be considered (Hof and Schuurmans, 2000). These dynamics can be described by the SV equations given in Eqs (1) and (2) for water transport and a one-dimensional AD equation given in Eq. (3) for salt transport.

$$\frac{\partial A}{\partial t} + \frac{\partial Q}{\partial x} = q_l \tag{1}$$

$$\frac{\partial Q}{\partial t} + \frac{\partial (Qu)}{\partial x} + gA\frac{\partial \varsigma}{\partial x} + g\frac{Q|Q|}{Cz^2 \cdot R \cdot A} = 0 \tag{2}$$

$$\frac{\partial (AC)}{\partial t} + \frac{\partial (QC)}{\partial x} = \frac{\partial}{\partial x}\left(KA\frac{\partial C}{\partial x}\right) + q_l C_l \tag{3}$$

where A is the cross sectional area [m^2], Q is the flow [m^3/s], q_l is the lateral inflow per unit length [m^3/s/m], u is the mean velocity (Q/A) [m/s], ς is the water depth above the reference plane [m], Cz = 40 is the Chezy coefficient [m$^{1/2}$/s], R is the hydraulic radius (A/P_f) [m], P_f is the wetted perimeter [m] and g is the gravity acceleration [m/s^2], K is the longitudinal dispersion coefficient [m^{2}s], C is the salt concentration [g/m^3], C_l is the lateral flow concentration [g/m^3], t is time [s] and x is horizontal length [m]. The longitudinal dispersion coefficient (K) is given by Fischer et al. (1979) as:

$$K = 0.011\frac{B^2 v^2}{d u_s} \tag{4}$$

where B is the mean width [m], d is the mean water depth [m], $u_s = (gRS_b)^{1/2}$ is the shear velocity [m/s], g is the gravitational acceleration (9.8 m/s^2), and S_b is the bottom slope of the canal [-]. The parameters used for discretization of the test ditch are given in Fig. 2.

These partial differential equations can be discretized using a staggered grid (Stelling and Duinmeijer, 2003) with a combination of

first order upwind and theta method for time integration. This discretization is explained in detail by Xu et al. (2010) thus will not be repeated here. The equations are implemented in MATLAB (The Mathworks Inc, 2016) to simulate the surface water system using initial conditions for the water level, concentrations and updated inflow and outflow discharges by the controller. For every simulation time step, the discretized SV equation calculates the water levels and velocities at the discretization points, followed by calculating the concentrations using the discretized AD equations.

The stability of the used models is important for a reliable control design and stable simulation of the system. In this study, we used a staggered grid discretization that is unconditionally stable (Stelling and Duinmeijer, 2003). The spatial discretization used in both simulation and control model is 10 m representing the drain spacing of the considered ditch. For the time discretization, 1 min time steps are used for the simulations and 2 min time steps are used for the controller. Normally, for testing the model performance of real time controllers the control time step can be much larger than the simulation time step; in this study we used a smaller control time step in order to capture the fast response of the controlled downstream water level and downstream salinity concentration to a change in flushing discharge because the length of the test polder ditch was only 100 m. In case of a longer ditch (where the travel time of the flushing water is much larger) the control time step can be selected to be appropriately larger. The second reason was to force the controller with a smaller control time step to illustrate that the computation time of control action is not a limitation for the scheme described in this paper. Computation time is discussed in Section 5.

3. Controller design

MPC is an optimization based control scheme which uses an internal model to predict the future process outputs within a specified prediction horizon (Camacho and Bordons, 2007). We used discretized SV and AD equations which serve as the internal model of the controller. Using the internal model equations, a time variant state space description (Eqn (5)) is obtained and used to describe and predict the states over the prediction horizon.

$$x(\,k+1\,) = A(k)x(k) + B(k)u(k) + B_d(k)d(k) \tag{5}$$

where x is the state vector of the system, u is the controlled variable, d is the disturbance and k is the discrete time step index. A, B and B_d are the time dependent matrices associated with system states, control input and disturbance input, respectively.

In the following paragraphs, the steps to achieve a time variant state space description for optimal flushing control is described and then the used objective function is defined. The controller controls the amount of flushing discharge, salinity and the water level at the downstream end of the polder ditch by manipulating the flushing and outflow discharges. According to the state space description given in Eqn (5); the states (x) are the water levels (h_i), concentrations (c_i), flushing discharge (Q_{flush}) and outflow discharge (Q_{out}) where i represents the discretization point in space; the inputs (u) are the change of flushing and outflow discharges (ΔQ_{flush}, ΔQ_{out}); and the disturbance (d) include all the remaining terms that are not associated with the states or inputs.

The internal model proposed uses the discretized SV and ADE as the basis. First, a discretization matrix is introduced that has similar terms like the state space description given in Eqn (5). At this stage, the water levels (h_i) and concentrations (c_i) are replaced with the deviation from water level set point ($eh_i = h_i\text{-}h_{ref}$) and deviation from concentration set point ($ec_i = c_i\text{-}c_{ref}$) since the controller aims to keep the water level and concentrations around the set point. Later, using algebraic operations, a state space description as Eqn (5) is achieved from the discretization matrix. Finally, additional states and inputs are introduced that are necessary for minimizing the freshwater usage.

3.1. Discretization matrix

Based on the discretization for SV and ADE given in Xu et al. (2010) and following a similar approach for combined open water quantity and quality model described in Xu et al. (2013), the discretized SV and AD equations are written in a compact matrix form including the flushing (Q_{flush}) and outflow discharges (Q_{out}) as the states and the change of these discharges (ΔQ_{flush},ΔQ_{out}) as the control input of the system. For the sake of simplicity, a discretization matrix with three discretization points is introduced here (Eqn (6)) and a general notation is provided in the Appendix. All the terms with the next time step (k+1) are written on the left side and the terms with the current time step (k) are left on the right side such that the states ($x(k+1)$ and $x(k)$), controlled variables ($u(k)$) and the disturbances ($d(k)$) in Eqn (5) are also present in the discretization matrix.

$$\begin{bmatrix} sv_{11} & sv_{12} & 0 & 0 & 0 & 0 & sv_f & 0 \\ sv_{21} & sv_{22} & sv_{23} & 0 & 0 & 0 & 0 & 0 \\ 0 & sv_{32} & sv_{33} & 0 & 0 & 0 & 0 & sv_o \\ 0 & 0 & 0 & ad_{11} & ad_{12} & 0 & ad_f & 0 \\ 0 & 0 & 0 & ad_{21} & ad_{22} & ad_{23} & 0 & 0 \\ 0 & 0 & 0 & 0 & ad_{32} & ad_{33} & 0 & ad_o \\ 0 & 0 & 0 & 0 & 0 & 0 & 1 & 0 \\ 0 & 0 & 0 & 0 & 0 & 0 & 0 & 1 \end{bmatrix}^{k+1} \begin{bmatrix} eh_1 \\ eh_2 \\ eh_3 \\ ec_1 \\ ec_2 \\ ec_3 \\ Q_{flush} \\ Q_{out} \end{bmatrix}^{k+1} =$$

$$\begin{bmatrix} 1 & 0 & 0 & 0 & 0 & 0 & 0 & 0 \\ 0 & 1 & 0 & 0 & 0 & 0 & 0 & 0 \\ 0 & 0 & 1 & 0 & 0 & 0 & 0 & 0 \\ 0 & 0 & 0 & ad_{11}^k & 0 & 0 & 0 & 0 \\ 0 & 0 & 0 & 0 & ad_{22}^k & 0 & 0 & 0 \\ 0 & 0 & 0 & 0 & 0 & ad_{33}^k & 0 & 0 \\ 0 & 0 & 0 & 0 & 0 & 0 & 1 & 0 \\ 0 & 0 & 0 & 0 & 0 & 0 & 0 & 1 \end{bmatrix}^{k} \begin{bmatrix} eh_1 \\ eh_2 \\ eh_3 \\ ec_1 \\ ec_2 \\ ec_3 \\ Q_{flush} \\ Q_{out} \end{bmatrix}^{k} + \begin{bmatrix} 0 & 0 \\ 0 & 0 \\ 0 & 0 \\ 0 & 0 \\ 0 & 0 \\ 0 & 0 \\ 1 & 0 \\ 0 & 1 \end{bmatrix} \begin{bmatrix} \Delta Q_{flush} \\ \Delta Q_{out} \end{bmatrix}^{k} + [I][d]^k \tag{6}$$

where sv_{ij}, ad_{ij} (i,j = 1:3), sv_f, sv_o, ad_f, ad_o and ad_{ij}^k (i,j = 1:3) are the time dependent terms from linearized equations associated with each state or control variable (see the Appendix for the details). To obtain these terms, every control time step, a pre-simulation of the system is conducted using the control variables of the optimization calculated at the previous control time step. This simulation is run for the entire prediction horizon such that the calculation of the water level and salinity concentration for every discretization point is conducted that will be used in the discretization matrix. These procedure is referred as forward estimation in Xu et al. (2010).

3.2. State space description

Equation (6) can be showed in a compact form as:

$$D_1x(k+1) = D_2x(k) + D_3u(k) + Id(k) \tag{7}$$

where D_1, D_2 and D_3 are compact forms of the corresponding matrices in Eqn (6). All the diagonal elements of D_1 are non-zeros, thus, the inverse of this matrix exists. After multiplying Eqn (7) with the inverse of D_1 matrix, the state space description given in Eqn (5) can be achieved with A ($D_1^{-1}D_2$), B ($D_1^{-1}D_3$) and Bd ($D_1^{-1}I$) matrices and the state space description is achieved as:

$$x(k+1) = D_1^{-1}D_2x(k) + D_1^{-1}D_3u(k) + D_1^{-1}Id(k) \tag{8}$$

This description relates the deviation of water level and the concentrations at the discretization points according to the change of flushing and outflow discharges and can be used only to control water level and salinity deviations from their set point. To achieve the third objective of minimization of freshwater use additional states and control variables are required and explained in the next section.

3.3. Objective function and constraints

Objective function is used to formulate the goals of the controller subject to the constrains of the system. The controller has to bring the states to their desired states by manipulating the control variables. Therefore, control actions also have to be considered in the objective function to limit the change of the control setting. In MPC formulation, the objective function is formulated as a quadratic function to deal with the positive and negative deviations from set points of the variables (van Overloop, 2006). A finite horizon objective function over the prediction horizon N_p with weighting matrices Q and R for states and the control variables respectively can be expressed as:

$$\min J = X^T Q X + U^T R U \tag{9}$$

The most important aspect of the developed control scheme in this study is to control water level and salinity by minimizing the freshwater use. To achieve that, the controller should limit itself to use freshwater only when it is necessary by flushing only if the salinity is above the given threshold and stop flushing when it is below the threshold. This can be achieved by introducing two soft constraints to the objective function. Soft constraints are used for variables that are allowed to violate their limitations (Maciejowski, 2002; van Overloop, 2006). Thus, they become active in the objective function only if they violate their limitations. For example, a soft constraint on flushing discharge with upper limit of 0 m^3/s will let the controller to violate this upper limit and use flushing if necessary. However, after the violation this use will be penalised by the objective function, thus, the controller will try to avoid this violation as much as possible.

Soft constraints are implemented as additional virtual input and virtual state variables into the system dynamics. Therefore, we used e^*_c to limit flushing only when the salinity concentration is below the set point and e^*_q to limit the amount of flushing. Virtual input has no physical meaning and it is subtracted from the state that needs to be constrained to achieve the virtual state. The objective function that is used in this study is given below:

$$\begin{aligned}
&\min J = \sum_{i=0}^{N_p} \{e_h(k+i|k)^T Q_{eh} e_h(k+i|k) + (e_c(k+i|k) - e_c^*)^T Q_{ec^*}(e_c(k+i|k) - e_c^*) \\
&+ (Q_{flush}(k+i|k) - e_q^*)^T Q_{eq^*}(Q_{flush}(k+i|k) - e_q^*)\Big\} \\
&+ \sum_{i=0}^{N_p-1} \{\Delta Q_{flush}(k+i|k)^T R_{\Delta Qflush} \Delta Q_{flush}(k+i|k) + \Delta Q_{out}(k+i|k)^T R_{\Delta Qout} \Delta Q_{out}(k+i|k) \\
&+ e_c^*(k+i|k)^T R_{ec^*} e_c^*(k+i|k) + e_q^*(k+i|k)^T R_{eq^*} e_q^*(k+i|k)\Big\}
\end{aligned}$$

subject to

$$\begin{bmatrix} x(k+1) \\ e_c(k+1) - e_c^* \\ Q_{flush}(k+1) - e_q^* \end{bmatrix} = \begin{bmatrix} A & 0 & 0 \\ A_6 & 0 & 0 \\ A_7 & 0 & 0 \end{bmatrix} \begin{bmatrix} x(k) \\ e_c(k) - e_c^* \\ Q_{flush}(k) - e_q^* \end{bmatrix} + \begin{bmatrix} B & 0 & 0 \\ B_6 & -1 & 0 \\ B_7 & 0 & -1 \end{bmatrix} \begin{bmatrix} u(k) \\ e_c^* \\ e_q^* \end{bmatrix} + \begin{bmatrix} B_d \\ B_{d6} \\ B_{d7} \end{bmatrix} \begin{bmatrix} d(k) \\ d_6(k) \\ d_7(k) \end{bmatrix}$$

$$\begin{aligned}
&e_h(k) = h(k) - h_{ref} \\
&e_c(k) = c(k) - c_{ref} \\
&h_{min} \le h_{ref} \le h_{max} \\
&-c_{ref} \le e_c^* \le 0 \\
&-Q_{flush}^{max} \le e_q^* \le 0 \\
&0 \le Q_{out} \le Q_{out}^{max} \\
&\Delta Q_{i,min} \le \Delta Q_i \le \Delta Q_{i,max}
\end{aligned} \tag{10}$$

where N_p is the prediction horizon; e_h and e_c are the water level and concentration deviations from set points at the last discretization point downstream of the polder ditch; e_c-e_c* and Q_{flush}-e_q* are the virtual states necessary for the soft constraints; Q_{eh}, Q_{ec}*, Q_{eq}* are the weights penalizing the corresponding states; $R_{\Delta Qflush}$, $R_{\Delta Qout}$, R_{ec^*} and R_{eq^*} are the weights penalizing the corresponding input variables; h_{ref} and c_{ref} are the water level and concentration set points at the last discretization point; Q_{flush}^{max} is the maximum capacity of flushing; Q_{out}^{max} is the maximum pumping capacity; ΔQ_i is the maximum allowed structure setting in a control time step for any control structure; h_{min} and h_{max} are the minimum and maximum allowed water levels. Updated state space description is also given here using the example given in Eqn (6) with three discretization points. A_6, A_7, B_6, B_7, B_{d6} and B_{d7} are the 6th or 7th rows of the original A, B and B_d matrices given in Eqn (8). Similarly, d_6 and d_7 are the 6th and 7th rows of the disturbance vector d.

4. Cases and scenarios

To test the proposed controller under different representative conditions, we apply it to three different exfiltration scenarios at two locations. For all scenarios, we control a simple one pool test polder ditch (Figs. 2–4) with a length of 100 m (the length of the ditch is selected such that it is representative of a small polder ditch and the length is not a limitation for the developed method). A spatial discretization spacing of 10 m is used for both simulations and the internal model calculations.

For the first two scenarios, we used exfiltration data from the Lissertocht catchment (Delsman et al., 2013). This catchment is a deep polder where the main salinity input is deep saline groundwater exfiltration through boils (de Louw et al., 2010). The drainage and ditch exfiltration salinity concentrations were calculated with RSGEM, leading to a mean of 75 g/m^3 and 336 g/m^3, respectively; boils have a mean salinity concentration of 5453 g/m^3 (Delsman et al., 2013). In the first scenario, we modelled and controlled a main channel directly collecting drainage water from the surrounding areas (Fig. 2). Saline groundwater exfiltration through the drains and ditches are modelled by RSGEM with daily time scales. We immediately represent the drain and ditch exfiltration modelled by RSGEM entering the test polder ditch. To test the controller, we selected a 24-day period (17 August

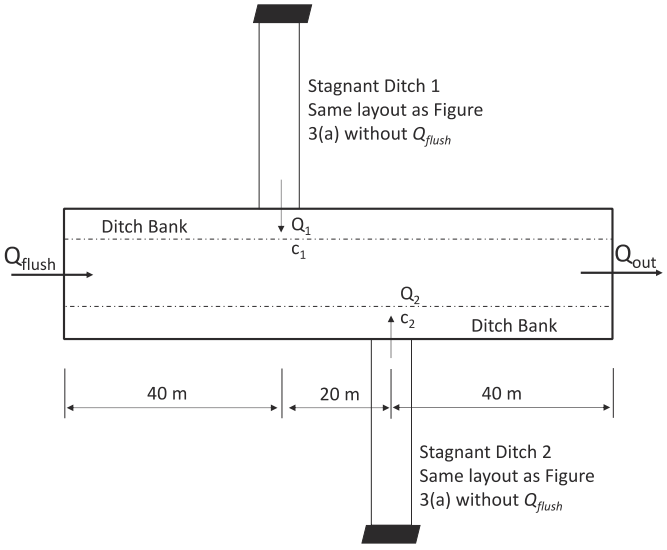

Fig. 3. Schematization of the test polder ditch (not to scale) for the second scenario with flushing discharge (Q_{flush}), outflow discharge (Q_{out}), outflow discharge ($Q_{1,2}$) (see Fig. 6b) and concentration ($c_{1,2}$) (see Fig. 6a) of the two stagnant ditches. The stagnant ditches have the same layout as the first scenario except no flushing discharge (shown as black block in this figure).

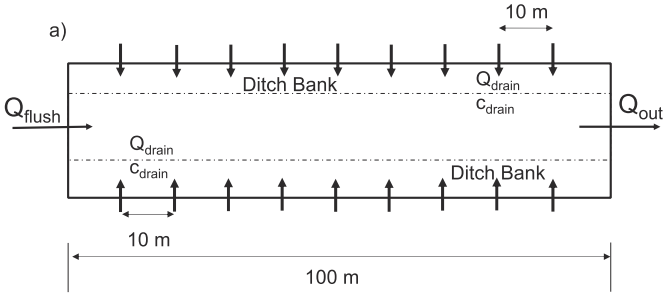

Fig. 4. Schematization of the test polder ditch (not to scale) for the third scenario with flushing discharge (Q_{flush}), outflow discharge (Q_{out}), drain exfiltration discharge (Q_{drain}) and concentration (c_{drain}).

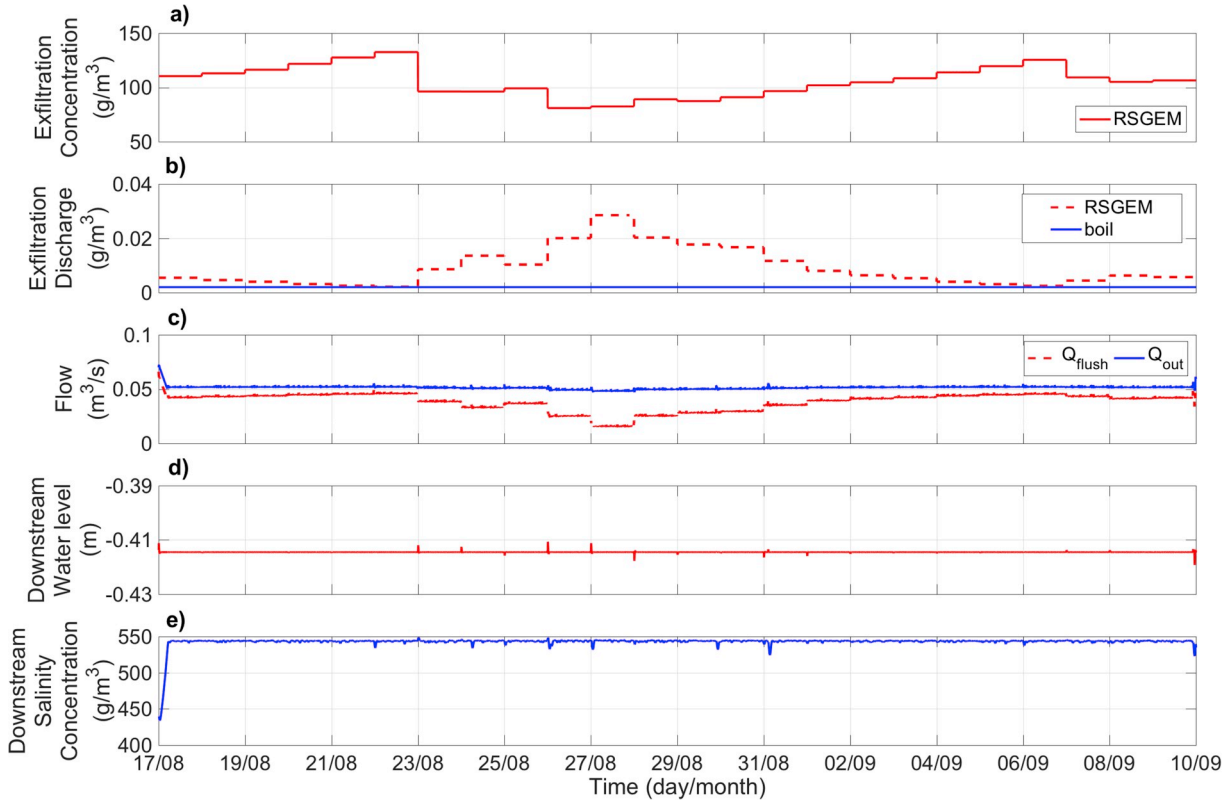

Fig. 5. Disturbance data and results of the controller for the first scenario. Groundwater exfiltration a) concentration (c_{boil} = 5453 g/m3 is constant and not shown in the figure) and b) discharge used for the first scenario (dashed lines shows the first location 40 m downstream of the flushing inlet which is a combination of the first boil and the exfiltration modelled by RSGEM and the solid line shows the second location which is 60 m downstream of the flushing inlet with the second boil only). c) Controlled flushing and outflow discharge, d) downstream water level and e) downstream salinity concentration.

2010–9 September 2010). In addition to the drain and ditch exfiltration modelled by RSGEM, two boils with a discharge of 0.002 m^3/s were added at locations 40 m and 60 m downstream of the flushing inlet. See Fig. 5a and b for the exfiltration concentrations and discharge, respectively, used in the first scenario.

In the second scenario, we illustrate the performance of the controller in case of stagnant ditches (that collects the drained water from the surrounding areas) connected to a main channel without drains, an often-occurring surface water layout in Dutch polders (Fig. 3). Some of the stagnant ditches with boils present in them are observed in Lissertocht catchment; they store high salt loads during dry periods. After an intensive rainfall event, these ditches are flushed naturally by the collected water from the drains. Therefore, in this scenario we first simulated the stagnant ditch for the same full dry period without an inflow discharge given in the first scenario and recorded the outflow discharge and concentrations at the end of the ditch every minute. We selected a test period with the highest surface water outflow salinity concentration and discharge for the simulations (8 April 2010–5 May 2010); these model inputs are shown in Fig. 6a and b, respectively. We assumed two stagnant ditches that are used to collect the drained water on the left and right banks of the polder ditch. The stagnant ditches are connected to the controlled main polder ditch at 40 m and 60 m downstream of the flushing inlet.

For the third scenario (Fig. 4), exfiltration data from a different polder is used (Schermer polder, location A in Fig. 1.). Contrary to the Lissertocht catchment, the main salinity input derives from shallow saline groundwater, exfiltrating towards ditches and tile drains. Tile drain and ditch exfiltration concentrations average 321 g/m^3 and 829 g/m^3 respectively and reach up to 5665 g/m^3 for both of them (Delsman et al., 2017). Using RSGEM, ditch and drain exfiltration discharge and concentration is modelled hourly and a test period with the highest salt load entering the system is selected (13–24 July 2012). See Fig. 7a and b for the ditch and drain exfiltration salinity concentration and discharge modelled by RSGEM, respectively.

For all three scenarios, drains with a spacing of 10 m are used to collect the excess water (fresh and saline groundwater) from the nearby areas. All of the ditches considered in this study have the same cross section as given in Fig. 2. The water level (h_{ref} = -0.41 m) and the salinity concentration (c_{ref} = 550 g/m^3) at the downstream end (last discretization point) of the ditch is controlled by manipulating flushing (Q_{flush}) and outflow (Q_{out}) discharges. The reference levels for water level and concentration are arbitrary and in the control calculation the deviations from the reference level are considered, therefore, they are not crucial for the method. A simulation time step of 1 min, a control time step of 2 min and a prediction horizon (N_p) of 30 steps (equal to 1-h prediction horizon) are used in the simulations. To determine the weights used in the objective functions, we used the maximum allowed value estimate approach described by van Overloop (2006) as an initial guess and arranged them accordingly as summarized in Table 1.

5. Results and discussions

5.1. Scenario 1

In this scenario, we used the proposed MPC scheme to control the test polder ditch with drains using the exfiltration data from Lissertocht catchment for 24-day period. In this catchment the main source of salinity is the boils. The drain and ditch exfiltration are fresh after a rain event because of the shallow freshwater lens in the catchment. This causes a decrease of modelled groundwater exfiltration concentration after 23/08 in Fig. 5a while the exfiltration discharge increases (Fig. 5b). This natural flushing due to rainfall is noticed by the

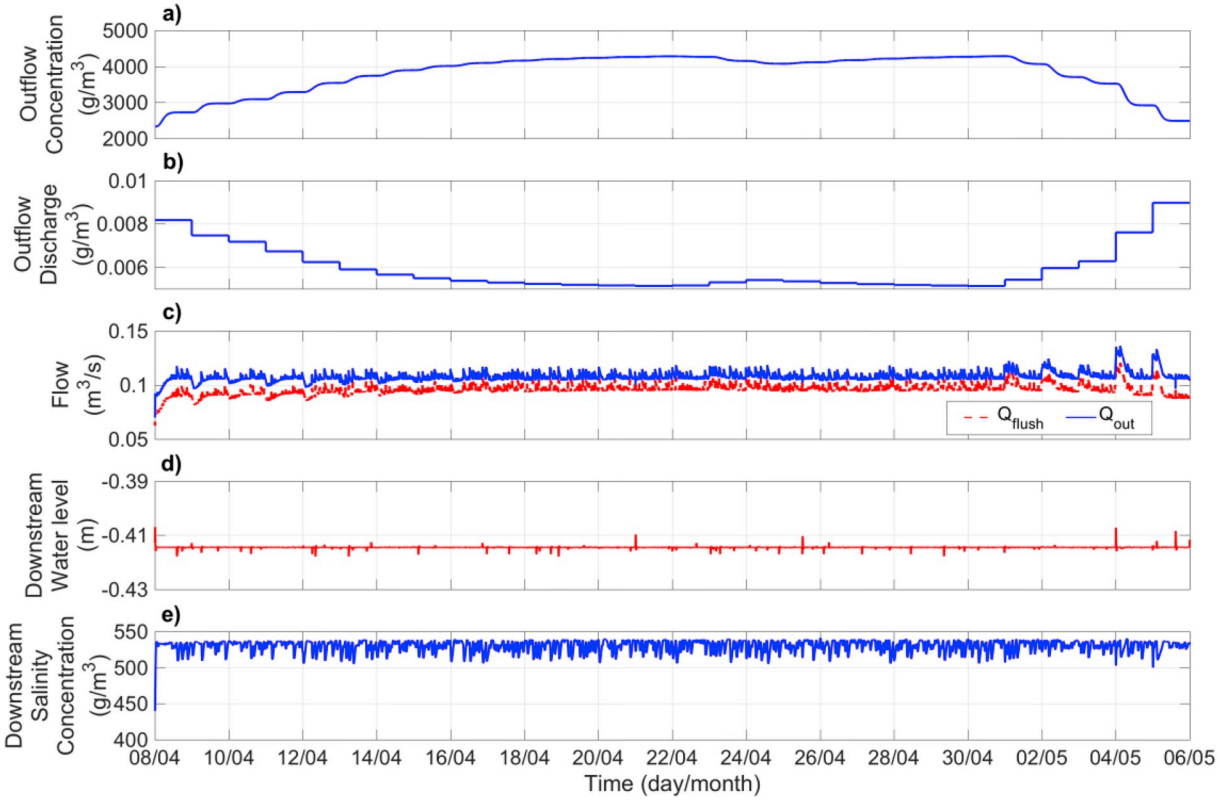

Fig. 6. Disturbance data and results of the controller for the second scenario. Surface water outflow a) concentration and b) discharge of the stagnant ditch connected to the controlled test polder ditch. c) Controlled flushing and outflow discharge, d) downstream water level, e) and downstream salinity concentration.

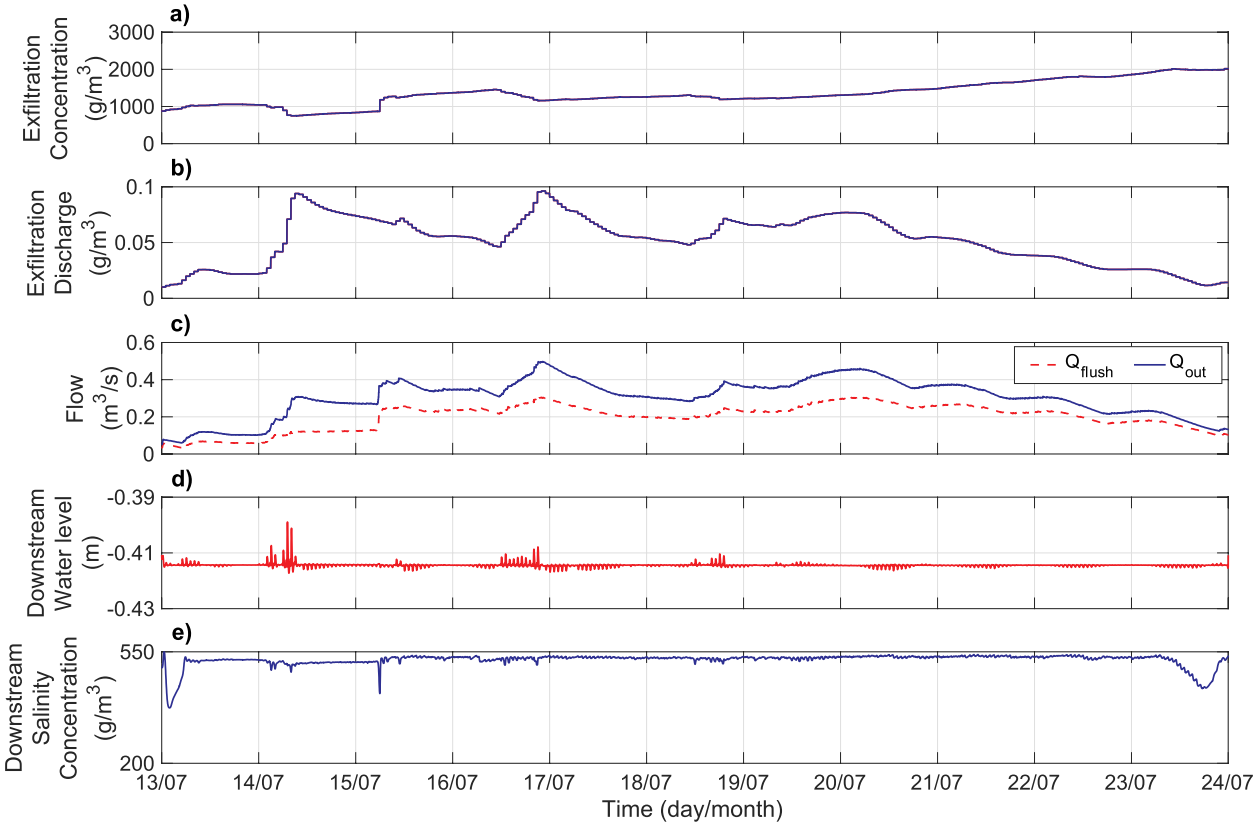

Fig. 7. Disturbance data and results of the controller for the third scenario. Groundwater exfiltration a) concentration and b) discharge used for the second scenario. c) Controlled flushing and outflow discharge, d) downstream water level, e) and downstream salinity concentration.

Table 1
Weights [-] used in the objective functions for the three scenarios.

	Qe_h	$Qe_c{}^*$,	$Qe_q{}^*$	$R_{\Delta Qflush}$	$R_{\Delta Qout}$	R_{ec^*}	R_{eq^*}
Scenario 1	16	62.5	0.01	80	80	10^{-4}	10^{-2}
Scenario 2	16	62.5	0.01	80	80	10^{-4}	10^{-2}
Scenario 3	16	6.25	0.01	4	4	10^{-4}	10^{-2}

controller, and it reduces the flushing during this time. The results of the MPC scheme can be seen in Fig. 5c–e.

As can be seen in Fig. 5c, the controller reacts to the groundwater exfiltration modelled by RSGEM (Fig. 5a and b) and keeps the water level (Fig. 5d) around the set point without any violation in salinity concentration (Fig. 5e). As expected, the controller anticipates the additional fresh drain water entering the ditch after 23/08 and reduces the flushing discharge (Q_{flush}) accordingly for this period, thus achieving the goal of flushing only when it is necessary.

5.2. Scenario 2

In this scenario, we wanted to see the effect of stagnant ditches connected to the main ditches in Lissertocht catchment. Stagnant ditches are used to collect the drained water and transfer it to the main channels. The upstream ends of the stagnant ditches are closed, and they are naturally flushed during the rainfall events resulting in an inflow to the main ditch (outflow from the stagnant ditch). There is no control structure in between, therefore, the water levels at the stagnant ditches also stays at the target value of the polder system. Similar saline groundwater exfiltration is modelled and simulated as the first scenario for two stagnant ditches without an inflow at the upstream end, using the water level at the connections as a boundary condition. The outflow discharge (Fig. 6a) and salinity concentrations (Fig. 6b) at the connections of the stagnant ditches to the controlled test polder ditch of the stagnant ditches (see Fig. 3) are simulated and used as a disturbance to the main channel controlled by the MPC scheme. Results are presented in Fig. 6c–e for a 28-day simulation.

As presented in Fig. 6c, the controller does not change the flushing discharge except for the small fluctuations throughout the simulation. This is due to the inverse relation between the exfiltration discharge and the concentration (Fig. 6a and b) resulting in a more or less constant salt load entering the system. Therefore, without a step change in flushing or outflow discharge the controller is able to keep the water level around the set point and the salinity concentration below the threshold.

5.3. Scenario 3

In the last scenario, we examined the performance of the controller in a polder with different saline groundwater exfiltration dynamics. Using data from the Schermer polder (with shallow saline groundwater), the MPC scheme is tested for a 11-day period. The results of the simulations are presented in Fig. 7c–e.

The results of this scenario show the ability of the proposed MPC scheme to deal with both increased exfiltration discharge fluxes (e.g. Fig. 7b after 14/07) and increased exfiltration concentration (e.g. Fig. 7a after 15/07). The initial salinity concentration is 500 g/m^3 at the downstream end of the ditch (Fig. 7e) while the exfiltration concentration is almost 1000 g/m^3 (Fig. 7a). The concentration drops below the threshold at the beginning of the simulation and the controller decreases the flushing until the controlled downstream concentration gets close to the threshold of 550 g/m^3. Moreover, as can be seen in Fig. 7c, the outflow discharge Q_{out} after 14/07 is increased while the flushing discharge Q_{flush} doesn't change considerably. This is due to the fact that the controller needs to pump the excess water out of the ditch while the current flushing is enough to keep the salinity concentration below the threshold. On the other hand, after 15/07 the controller introduces additional freshwater into the system by a step increase of flushing discharge Q_{flush}. The outflow discharge is adjusted with a similar increase to keep the water level at set point. With similar arrangements on flushing and outflow discharges the controller keeps the water level (Fig. 7d) and concentration (Fig. 7e) in accordance with the objective of the controller. Moreover, as can be seen clearly after 20/07, the flushing and outflow discharges are decreased, as the saline groundwater exfiltration after this point requires less freshwater to achieve the salinity concentration control objective. This shows that the third objective of the controller to use a minimum of freshwater is also achieved.

To demonstrate how much freshwater and pumping water can be saved by using the developed control scheme, we compared results of the simulations with different salinity concentration to the current fixed flushing practice. We did the analysis only for the third scenario due to its high dependency on exfiltration dynamics. We assumed the maximum flushing discharge achieved during the simulations using the proposed MPC scheme is the maximum capacity of the intake of the test polder ditch and used this as the fixed flushing discharge for comparison. The results are presented in Table 2.

For all the simulations presented in Table 2, similar results are obtained as in Fig. 7. Flushing with MPC kept the salinity level close to the set point without any violations and the water level was always around the set point with fluctuations within the range of maximum and minimum water levels defined in the objective function. As can be seen in Table 2, increasing salinity set points resulted in less need for flushing discharge. Although in this study we used a given fixed threshold for the salinity concentration over the whole simulation period, in practice the concentration requirement will be varying, depending on the requirements. With a known but spatially and temporally varying demand for quantity and quality, the developed MPC scheme can be modified such that the demand is satisfied using the predictive behavior of the controller. By this way additional savings in freshwater and pumping use can be achieved. Simulations with fixed flushing always resulted in more flushing and pumping than the flushing with MPC. More than 35% savings in freshwater use is achieved by using the proposed MPC scheme. Similarly, the savings in total pumping volume reached up to 36% in case of using MPC. With fixed flushing, the average salinity concentration over the simulation period is below the set point which results in a better water quality. However, as discussed earlier this is due to the unwanted excessive freshwater usage, resulting in unnecessary pumping and energy use.

Using a discretized internal model (as opposed to an internal model achieved by model reduction as proposed by Xu et al. (2013)) is also an

Table 2
Comparison between flushing with MPC and current practice of fixed flushing with different salinity threshold.

C_{ref} (g/m^3)	C_{av} (g/m^3)		Q_{max} (m^3/s)	Σ Q_{flush} (10^3 m^3)		Σ Q_{pump} (10^3 m^3)		% Saved	
	MPC	Fixed	MPC	MPC	Fixed	MPC	Fixed	Q_{flush}	Q_{pump}
550	512.8	374.2	0.384	198.1	365.2	296.8	463.9	45.7	36.0
750	684.9	555.2	0.172	105.6	163.4	204.3	262.0	35.3	22.0
900	810.8	664.8	0.115	67.7	109.2	166.4	207.9	38.0	19.9
1000	893.7	714.7	0.096	49.2	91.6	147.9	190.2	46.2	22.2

important outcome of this research which will give the operator to modify the controller such that the water level and the salinity concentration can be controlled in any discretization points. In this study we used 10 m discretization spacing for the internal model, resulting in total of 24 states and 4 control variables. We used a control time step of 2 min with 1-h prediction horizon (i.e. 30 control time steps) resulting in total of 24*30 states and 4*30 control variables, respectively. To illustrate the computational time, one closed loop simulation (calculation of control actions over the whole prediction horizon followed by simulation of the system dynamics with the calculated control action) ended in less than 0.1 s. All the computations performed within MATLAB R2017a-64 bit for macOS High Sierra (v 10.13.6) installed on a 2.9 GHz Intel Core i5. In a polder system without any intermediate structures between the ditches, the network of ditches is controlled by the intake structures and the pumps in the system only. However, a farmer can use the water in any intermediate location without a hydraulic structure, and therefore, this feature can be interesting by means of salinity and water availability. The flexibility of controlling the main structures according to the states of any intermediate location is an important outcome of the developed MPC scheme.

6. Conclusion and future work

In this study, a MPC scheme was developed for optimizing flushing of a polder catchment. We provided a MPC scheme to control the salinity concentration and water level in a polder ditch also considering the freshwater usage. We tested the scheme on a test polder ditch layout. The controller was numerically tested for different scenarios and compared with the current operation practice in the field. The results showed that MPC of flushing of a polder ditch results in savings in the order of 35–45% freshwater use, depending on the salinity thresholds.

RSGEM is used to estimate the exfiltration flux and concentration for a realistic scenario using past data. However, this is not a limitation for the controller. The weather predictions and estimations of related events can be used to run the fast RSGEM as a predictive model with required uncertainty assessments and the developed MPC scheme can be used in real time.

Although in this study we focused on salinity as the source of water quality problem, other nutrients that are used in the fields and accumulated in the ditches by means of drained water can also be controlled with the developed MPC scheme. The limitation in such a control scheme will be obtaining real time measurements for the nutrient levels in the ditches.

For future research, we will apply the developed controller to the whole water course network of the Lissertocht catchment. With multiple inlets and pumping stations, a network of ditches without control structures in between, higher saline groundwater exfiltration through boils from different locations, applying MPC to the flushing operation of the Lissertocht catchment will be challenging and interesting. Moreover, uncertainties of the system and the predictions are to be addressed.

The dependency between the water used and energy consumed is an important issue, often referred to as ‘water-energy nexus’ (Bazilian et al., 2011; Siddiqi and Anadon, 2011), and needs to be considered for sustainable future planning. The relation between the flushing and corresponding energy consumption will be introduced to the optimization of the developed control scheme. This will enable the operators to manipulate the flushing of the polders in a sustainable manner.

Acknowledgement

This research is financed by the Netherlands Organisation for Scientific Research (NWO), which is partly funded by the Ministry of Economic Affairs and Climate Policy, and co-financed by the Netherlands Ministry of Infrastructure and Water Management and partners of the Dutch Water Nexus consortium.

Appendix A. Supplementary data

Supplementary data to this article can be found online at https://doi.org/10.1016/j.envsoft.2018.11.010.

Appendix

SV and AD equations are discretized following (Xu et al., 2010) using a staggered grids. A discretization matrix (See Equation (6)) for n discretization points is obtained with the terms given as:

For i = 1

$$sv_{i,i} = 1 + \frac{\Delta t}{A_{s,i}^{n}} A_i^{k} fu_{i+1/2}\; sv_{i,i+1} = -\frac{\Delta t}{A_{s,i}^{k}} A_i^{k} fu_{i+1/2}\; sv_f = -\frac{\Delta t}{A_{s,i}^{n}}\; d_i = -\frac{\Delta t}{A_{s,i}^{k}} A_i^{k}\, ru_{i+1/2} + \frac{\Delta t Q_{l,i}^{k}}{A_{s,i}^{k}}$$

$$ad_{i,i} = 1 + \frac{\Delta t}{V_i^{k}}\left(\frac{1}{\Delta x}\left(K_{i+1/2}^{k+1} A_{i+1/2}^{k+1} + K_{in}^{k+1} A_i^{k+1}\right) + Q_{i+1/2}^{k+1}\right)\; ad_{i,i+1} = -\frac{\Delta t}{V_i^{n}.\Delta x} K_{i+1/2}^{k+1} A_{i+1/2}^{k+1}\; ad_f = \frac{\Delta t}{V_i^{k}}\left(C_i^{k} - C_{in}^{k+1}\right)\; ad_{i,i}^{k} = 1 + \frac{\Delta t\left(Q_{i+1/2}^{k+1}\right)}{V_i^{k}}\; d_{i+n}$$
$$= \frac{\Delta t}{V_i^{n}}\left(\frac{1}{\Delta x} K_{in}^{k+1} A_i^{k+1}\right)\left(C_{in}^{k+1} - c_{ref}\right) + \frac{Q_{l,i}^{k} \Delta t\left(C_{l,i}^{n} - C_i^{n}\right)}{V_i^{n}}$$

For i = 2:n-1

$$sv_{i,i} = 1 + \frac{\Delta t}{A_{s,i}^{k}} A_{i-1}^{k} fu_{i-1/2} + \frac{\Delta t}{A_{s,i}^{k}} A_i^{k} fu_{i+1/2}\; sv_{i,i-1} = -\frac{\Delta t}{A_{s,i}^{k}} A_{i-1}^{k} fu_{i-1/2}\; sv_{i,i+1} = -\frac{\Delta t}{A_{s,i}^{k}} A_i^{k} fu_{i+1/2}\; d_i = \frac{\Delta t}{A_{s,i}^{k}} A_{i-1}^{k}\left(ru_{i-1/2}\right) - \frac{\Delta t}{A_{s,i}^{k}} A_i^{k}\left(ru_{i+1/2}\right) + \frac{\Delta t Q_{l,i}^{k}}{A_{s,i}^{k}}$$

$$ad_{i,i} = 1 + \frac{\Delta t}{V_i^{k}}\left(\frac{1}{\Delta x}\left(K_{i+1/2}^{k+1} A_{i+1/2}^{k+1} + K_{i-1/2}^{k+1} A_{i-1/2}^{k+1}\right) + Q_{i+1/2}^{k+1}\right)\; ad_{i,i-1} = -\frac{\Delta t}{V_i^{k}}\left(\frac{1}{\Delta x} K_{i+1/2}^{k+1} A_{i-1/2}^{k+1} + Q_{i-1/2}^{k+1}\right)\; ad_{i,i+1} = -\frac{\Delta t}{V_i^{k}} \frac{1}{\Delta x} K_{i+1/2}^{k+1} A_{i+1/2}^{k+1}\; ad_{i,i}^{k}$$
$$= 1 + \frac{\Delta t\left(\left(Q_{i+1/2}^{k+1}\right) - \left(Q_{i-1/2}^{k+1}\right)\right)}{V_i^{k}}\; d_{i+n} = \frac{Q_{l,i}^{k} \Delta t\left(C_{l,i}^{k} - C_i^{k}\right)}{V_i^{k}}$$

For i = n

$$sv_{i,i} = 1 + \frac{\Delta t}{A_{s,i}^k} A_{i-1}^k fu_{i-1/2}\ sv_{i,i-1} = -\frac{\Delta t}{A_{s,i}^k} A_{i-1}^k fu_{i-1/2}\ sv_o = \frac{\Delta t}{A_{s,i}^k}\ d_i = \frac{\Delta t}{A_{s,i}^k} \theta A_{i-1}^k (ru_{i-1/2}) + \frac{\Delta t Q_{l,i}^k}{A_{s,i}^k}$$

$$ad_{i,i} = 1 + \frac{\Delta t}{V_i^k}\left(\frac{1}{\Delta x}\left(K_{i-1/2}^{k+1} A_{i-1/2}^{k+1}\right)\right) ad_{i,i-1} = -\frac{\Delta t}{V_i^k}\left(\frac{1}{\Delta x} K_{i-1/2}^{k+1} A_{i-1/2}^{k+1} + Q_{i-1/2}^{k+1}\right) ad_o = \frac{\Delta t}{V_i^k}\left(C_i^{k+1} - C_i^k\right)$$

$$ad_{l,i}^k = 1 - \frac{C_i^k \Delta t (Q_{i-1/2}^{k+1})}{V_i^n}\ d_{i+n} = \frac{Q_{l,i}^k \Delta t (C_{l,i}^k - C_i^k)}{V_i^n}$$

Where $fu_{i+1/2}^k = \frac{g\Delta t}{\Delta x\left(1 + g\frac{v_{i+1/2}^k}{Cz^2 R}\right)}$, $ru_{i+1/2}^k = \frac{\frac{1}{A_{i+1/2}^k}\left(\frac{\bar{Q}_{i+1}^k v_{i+1/2}^k - \bar{Q}_i^k v_{i-1/2}^k}{\Delta x} + v_{i+1/2}^k \frac{Q_{i+1}^k - Q_i^k}{\Delta x}\right) + v_{i+1/2}^k}{\left(1 + g\frac{v_{i+1/2}^k}{Cz^2 R}\right)}$, $\bar{Q}_i^k = (Q_{i+1/2}^k - Q_{i+1/2}^k)/2\ \bar{A}_{i+1/2}^k = (A_{i+1/2}^k - A_{i+1/2}^k)/2$, K_{in} and C_{in} are the dispersion coefficient and the concentration of the incoming water.

References

Augustijn, D.C.M., van den Berg, M., de Bruine, E., Korving, H., 2011. Dynamic control of salt intrusion in the mark-vliet river system, The Netherlands. Water Resour. Manag. 25, 1005–1020. https://doi.org/10.1007/s11269-010-9738-1.

Aydin, B.E., van Overloop, P.J., Rutten, M., Tian, X., 2016. Offset-Free model predictive control of an open water channel based on moving horizon estimation. J. Irrigat. Drain. Eng., B4016005. https://doi.org/10.1061/(ASCE)IR.1943-4774.0001085.

Bautista, E., Strelkoff, T.S., Clemmens, A.J., 2003. General characteristics of solutions to the open-channel flow, feedworward control problem. J. Irrig. Drain. Eng. 129, 129–137.

Bazilian, M., Rogner, H., Howells, M., Hermann, S., Arent, D., Gielen, D., Steduto, P., Mueller, A., Komor, P., Tol, R.S.J., Yumkella, K.K., 2011. Considering the energy, water and food nexus: towards an integrated modelling approach. Energy Pol. 39, 7896–7906. https://doi.org/10.1016/j.enpol.2011.09.039.

Camacho, E., Bordons, C., 2007. Model predictive control. In: Advanced Textbooks in Control and Signal Processing, second ed. Springer London, London. https://doi.org/10.1007/978-0-85729-398-5.

Cho, J.H., Seok Sung, K., Ryong Ha, S., 2004. A river water quality management model for optimising regional wastewater treatment using a genetic algorithm. J. Environ. Manag. 73, 229–242. https://doi.org/10.1016/j.jenvman.2004.07.004.

Clemmens, a. J., Wahlin, B.T., 2004. Simple optimal downstream feedback canal controllers: ASCE test case results. J. Irrig. Drain. Eng. 130, 35–46. https://doi.org/10.1061/(ASCE)0733-9437. 130:1(35).

de Louw, P.G.B., Oude Essink, G.H.P., Stuyfzand, P.J., van der Zee, S.E.A.T.M., 2010. Upward groundwater flow in boils as the dominant mechanism of salinization in deep polders, The Netherlands. J. Hydrol. 394, 494–506. https://doi.org/10.1016/j.jhydrol.2010.10.009.

de Louw, P.G.B., Vandenbohede, A., Werner, A.D., Oude Essink, G.H.P., 2013. Natural saltwater upcoming by preferential groundwater discharge through boils. J. Hydrol. 490, 74–87. https://doi.org/10.1016/j.jhydrol.2013.03.025.

Delgoda, D., Malano, H., Saleem, S.K., Halgamuge, M.N., 2016. Irrigation control based on model predictive control (MPC): formulation of theory and validation using weather forecast data and AQUACROP model. Environ. Model. Softw. 78, 40–53. https://doi.org/10.1016/j.envsoft.2015.12.012.

Delsman, J.R., 2015. Saline groundwater-Surface water interaction in coastal lowlands. In: Saline Groundwater - Surface Water Interaction in Coastal Lowlands. IOS Press, Inc., Amsterdam. https://doi.org/10.3233/978-1-61499-518-0-i.

Delsman, J.R., de Louw, P.G.B., de Lange, W.J., Oude Essink, G.H.P., 2017. Fast calculation of groundwater exfiltration salinity in a lowland catchment using a lumped celerity/velocity approach. Environ. Model. Softw. 96, 323–334. https://doi.org/10.1016/j.envsoft.2017.07.004.

Delsman, J.R., Hu-A-Ng, K.R.M., Vos, P.C., De Louw, P.G.B., Oude Essink, G.H.P., Stuyfzand, P.J., Bierkens, M.F.P., 2014a. Paleo-modeling of coastal saltwater intrusion during the Holocene: an application to The Netherlands. Hydrol. Earth Syst. Sci. 18, 3891–3905. https://doi.org/10.5194/hess-18-3891-2014.

Delsman, J.R., Oude Essink, G.H.P., Beven, K.J., Stuyfzand, P.J., 2013. Uncertainty estimation of end-member mixing using generalized likelihood uncertainty estimation (GLUE), applied in a lowland catchment. Water Resour. Res. 49, 4792–4806. https://doi.org/10.1002/wrcr.20341.

Delsman, J.R., Waterloo, M.J., Groen, M.M.A., Groen, J., Stuyfzand, P.J., 2014b. Investigating summer flow paths in a Dutch agricultural field using high frequency direct measurements. J. Hydrol. 519, 3069–3085. https://doi.org/10.1016/j.jhydrol.2014.10.058.

Delta Programme Commissioner, 2014. Delta Programme 2015 - Working on the Delta - the Decisions to Keep the Netherlands Safe and Liveable.

Fischer, H.B., List, E.J., Koh, R.C.Y., Imberger, J., Brooks, N.H., 1979. Mixing in Inland and Coastal Waters, Mixing in Inland and Coastal Waters. Elsevierhttps://doi.org/10.1016/C2009-0-22051-4.

Forzieri, G., Feyen, L., Rojas, R., Flörke, M., Wimmer, F., Bianchi, a., 2014. Ensemble projections of future streamflow droughts in Europe. Hydrol. Earth Syst. Sci. 18, 85–108. https://doi.org/10.5194/hess-18-85-2014.

Fu, G., Butler, D., Khu, S.-T., 2008. Multiple objective optimal control of integrated urban wastewater systems. Environ. Model. Softw. 23, 225–234. https://doi.org/10.1016/j.envsoft.2007.06.003.

Hof, A., Schuurmans, W., 2000. Water quality control in open channels. Water Sci. Technol. 42, 153–159.

Horváth, K., Galvis, E., Valentín, M.G., Rodellar, J., 2015. New offset-free method for model predictive control of open channels. Contr. Eng. Pract. 41, 13–25. https://doi.org/10.1016/j.conengprac.2015.04.002.

Klijn, F., Van Velsen, E., Ter Maat, J., Hunink, J.C., 2012. Zoetwatervoorziening in Nederland. in Dutch).

Litrico, X., Belaud, G., Fovet, O., 2011. Adaptive control of algae detachment in regulated canal networks. In: 2011 Int. Conf. Networking, Sens. Control. ICNSC 2011, pp. 197–202. https://doi.org/10.1109/ICNSC.2011.5874878.

Maciejowski, J.M., 2002. Predictive Control with Constraints. Prentice Hall, New York.

Oude Essink, G.H.P., Van Baaren, E.S., De Louw, P.G.B., 2010. Effects of climate change on coastal groundwater systems: a modeling study in The Netherlands. Water Resour. Res. 46, 1–16. https://doi.org/10.1029/2009WR008719.

Puig, V., Romera, J., Quevedo, J., Sarrate, R., Morales-Hernandez, M., Gonzalez-Sanchis, M., Garcia-Navarro, P., 2014. Automatic control of pollutant on a shallow river using surface water systems: application to the Ebro River. Water Sci. Technol. 69, 2210–2220. https://doi.org/10.2166/wst.2014.140.

Schuurmans, J., 1997. Control of Water Levels in Open Channels (PhD Dissertation). Delft Univesity of Technology, The Netherlands.

Schuurmans, J., Bosgra, O.H., Brouwer, R., 1995. Open-channel flow model approximation for controller design. Appl. Math. Model. 19, 525–530. https://doi.org/10.1016/0307-904X(95)00053-M.

Siddiqi, A., Anadon, L.D., 2011. The water-energy nexus in Middle East and North Africa. Energy Pol. 39, 4529–4540. https://doi.org/10.1016/j.enpol.2011.04.023.

Stelling, G.S., Duinmeijer, S.P. a, 2003. A staggered conservative scheme for every Froude number in rapidly varied shallow water flows. Int. J. Numer. Methods Fluid. 43, 1329–1354. https://doi.org/10.1002/fld.537.

The Mathworks Inc, 2016. MATLAB - MathWorks [WWW Document]. doi:2016-11-26. www.mathworks.com/products/matlab.

Tian, X., Aydin, B.E., Negenborn, R.R., van de Giesen, N., Maestre, J.M., 2016. Model predictive control for water level control in the case of spills. J. Irrig. Drain. Eng. 143, B4016006. https://doi.org/10.1061/(ASCE)IR.1943-4774.0001133.

Tian, X., Negenborn, R.R., van Overloop, P.-J., María Maestre, J., Sadowska, A., van de Giesen, N., 2017. Efficient multi-scenario model predictive control for water resources management with ensemble streamflow forecasts. Adv. Water Resour. 109, 58–68. https://doi.org/10.1016/j.advwatres.2017.08.015.

van Overloop, P.-J., 2006. Model Predictive Control on Open Water Systems. Delft University of Technology, The Netherlands.

van Overloop, P.J., Horváth, K., Aydin, B.E., 2014. Model predictive control based on an integrator resonance model applied to an open water channel. Contr. Eng. Pract. 27, 54–60. https://doi.org/10.1016/j.conengprac.2014.03.001.

Xu, M., 2016. Model predictive control of an irrigation canal using dynamic target trajectory. J. Irrig. Drain. Eng. 143, B4016004. https://doi.org/10.1061/(ASCE)IR.1943-4774.0001084.

Xu, M., van Overloop, P.J., van de Giesen, N.C., 2013. Model reduction in model predictive control of combined water quantity and quality in open channels. Environ. Model. Softw. 42, 72–87. https://doi.org/10.1016/j.envsoft.2012.12.008.

Xu, M., Van Overloop, P.J., Van De Giesen, N.C., Stelling, G.S., 2010. Real-time control of combined surface water quantity and quality: polder flushing. Water Sci. Technol. 61, 869–878. https://doi.org/10.2166/wst.2010.847.